IEEE Open Journal of the
Industrial Electronics Society

Received 4 December 2023; accepted 12 January 2024. Date of publication 16 January 2024;
date of current version 31 January 2024. The review of this paper was arranged by Associate Editor Giampaolo Buticchi.

Digital Object Identifier 10.1109/OJIES.2024.3354799

On the Detection of Neutral Loss, Islanding, and Meter Tampering in Electrical Installations

SYLLAS FRANTZESKAKIS[1], NICK RIGOGIANNIS[1] (Member, IEEE), CHRISTOS CHRISTODOULOU[2], AND NICK PAPANIKOLAOU[1] (Senior Member, IEEE)

[1]Department of Electrical and Computer Engineering, Democritus University of Thrace, GR-67131 Xanthi, Greece
[2]School of Electrical and Computer Engineering, National Technical University of Athens, GR-15780 Athens, Greece

CORRESPONDING AUTHOR: NICK PAPANIKOLAOU (e-mail: npapanik@ee.duth.gr)

This work was supported in part by the European Regional Development Fund of the European Union and in part by Greek National Funds through the Operational Program East Macedonia and Thrace 2014-2020, under the call "Investment Plans for Innovation, Research and Development of Companies in the Branch of Electronics and Electrical Equipment Production" (Project code: AMTH3-0063343).

ABSTRACT Neutral conductor loss on the upstream network of an electrical installation, as well as unintentional islanding operation, are two critical issues directly related to the safety of both human life and equipment of the electrical installation. Furthermore, another critical issue is meter tampering, which affects the operation and development of national power sectors. The state-of-the-art methods deal with those issues separately, without providing a holistic solution; moreover, they are facing several challenges in the prospect of mass storage installations at buildings. This article introduces a new scheme for the detection of neutral loss at the upstream network, the unintentional islanding conditions, and meter tampering simultaneously. In this context, a suitable technical solution is given by using one low-power H-bridge inverter and a current transformer, along with voltage and current measuring instruments. The detection scheme is based on the injection of a (zero-sequence) 12th harmonic voltage component in series with the utility voltage and the monitoring of the corresponding harmonic current component. The theoretical analysis of the proposed technique is discussed, whereas its effectiveness is validated through simulation and experimental results.

INDEX TERMS Harmonics, impedance estimation, inverter, islanding detection, neutral loss, meter tampering.

I. INTRODUCTION

The massive penetration of distributed energy resources (DERs) in modern electrical infrastructure, along with the forthcoming mass installations of energy storage units [1], [2], calls for a detection scheme that can diagnose the faulty conditions in an electrical installation (i.e., unintentional islanding operation and neutral conductor loss). Apparently, it is expected that such a detection scheme is going to be mandatory in the near future, due to the increasing frequency of matching load condition cases that will occur in the prospect of zero energy building (ZEB) and vehicle-to-grid (V2G) concepts.

Apparently, due to the fact that future ZEBs will have to serve considerably higher amounts of electric loads (for heating and cooling purposes, electric vehicle charging, etc.) and the fact that the relevant EU directives [2] impose the mass installation of battery units in buildings (in order to reduce energy transactions with the public grids), it is concluded that future ZEBs will have more balanced loads (i.e., in terms of local production and demand).

In more detail, the recent EU policies [3] demand the transformation of the Building Sector into a highly efficient, zero energy consumer, aiming at the gradual independence of (imported and environmentally aggravating) carbon-based fossil fuels. Hence, the Building Sector becomes an extended, distributed Prosumer, where energy production, consumption, and storage units are incorporated. This is a completely new architecture and operational principle for the public grids, raising some challenges regarding, protection, power quality, and energy management [4], [5]. Under this light, the–more or less–effectively dealt protection issues against islanding and loss of neutral are coming back in more intense.

© 2024 The Authors. This work is licensed under a Creative Commons Attribution-NonCommercial-NoDerivatives 4.0 License. For more information, see https://creativecommons.org/licenses/by-nc-nd/4.0/

According to the relevant scientific literature [6], [7], [8], the most popular active anti-islanding protection schemes are based on the urge of some sort of disturbance (either in voltage amplitude or frequency, or harmonic distortion) and a positive feedback loop, so as to force the islanded network to collapse. However, the effectiveness of this disturbance loop is subject to the quality factor, QF, of the islanded network; hence, the relevant Standards [9], [10] foresee a maximum QF value equal to unity. Moreover, it is evident that most commercial anti-islanding algorithms are designed without considering the presence of multiple distributed generators (DGs) at the same point of common coupling (PCC). Although those assumptions are rational for grids with limited presence of DGs and energy storage units, this situation is about to change; the transformation of the Building Sector into ZEB, implies mass installations of multiple DGs and storage units at the same PCC, whereas the applied building energy management schemes will focus on the minimization of energy transactions with the public electricity networks. Thus, the ZEB installations will face matching load conditions for extended time periods (unlike what is the present status). Furthermore, the presence of energy storage corresponds to a drastic increase in their equivalent QF-value (due to the ability of the energy storage to absorb any voltage disturbances and/or energy unbalances). Those facts are jeopardizing the effectiveness of current anti-islanding techniques, creating so a gap in anti-islanding protection of ZEBs. What is more, the incorporation of V2G concept is expected to widen this protection gap, due to its contribution to the energy storage capacity of the building [11].

The aforementioned changes in the features of building electrical installations have also a serious impact on the protection schemes against loss of neutral. Although such a faulty condition is effectively detected by conventional relays in conventional installations, their operational efficacy is jeopardized by the forthcoming mass installations of multiple DGs and storage units at buildings, as it has been already discussed in [1] and [2]. Last but not least, the issue of meter tampering in building electrical installations is a well-known problem; based on a related study by Northeast Group LLC, power theft worldwide amounts to USD 96 billion, annually. It is indicative that at the national level, the Hellenic Distribution Network Operator, according to official data regarding the nontechnical losses of the Distribution Network, estimates that the cost of stolen energy is roughly EUR 80 million per year.

The above protection challenges in building installations have not been adequately discussed in the relevant literature, under the prospect of the forthcoming mass penetration of multiple DGs and storage units at buildings, leaving so a technical gap regarding the safe operation of ZEBs. In light of this, the main contribution of the current work is the proposal of an active method that is capable of detecting faulty conditions in electrical installations, such as unintentional islanding operation and neutral conductor loss, regardless of the penetration level of DGs, the types of their grid-tie inverters and the presence of storage units. Moreover, the same method is capable to detect any activity to tamper the electric energy meter, providing a global solution for the safe and reliable operation of ZEBs. The proposed active detection method will be theoretically discussed in the following paragraphs, whereas simulations and experimental results at a laboratory test bench will validate its effectiveness.

II. STATE-OF-THE-ART METHODS FOR DETECTING ISLANDING OPERATION, NEUTRAL CONDUCTOR LOSS, AND ELECTRICAL METER TAMPERING

As it has been already discussed, the state-of-the-art methods (which are presented in this section) regarding the detection of unintentional islanding, neutral conductor loss, and meter tampering, feature only standalone detection schemes for the protected installation, rather than a universal protection scheme.

A. NEUTRAL CONDUCTOR LOSS

Neutral conductor loss is a critical issue for the electrical installations, since it is directly related to the safety of both human life and the electrical installation. The interruption may occur due to poor maintenance, poor connection at the electric poles, or even stolen neutral bus conductors [12]. The interruption of a neutral conductor at the upstream network of an installation is a known issue, yet not fully addressed in view of the forthcoming massive installation of DG and storage units (including the V2G concept). Such a condition may result in serious repercussions for the connected electrical installations and the consumers [13]. The consequences of a lost neutral conductor depend mainly on the load balance conditions in a three-phase (3 ph) system, but also on the type of the earthing system that is used and the point of the neutral interruption (relatively to the load location). It is noted that the relevant Standards (e.g., IEC 60364) do not deal with the protection of installations against neutral loss [9]; neither residual current devices nor earthing systems are capable of protecting both human and the equipment under such a circumstance.

A device that is capable of passively detecting the loss of neutral conductor is the voltage monitoring device [15]. Once the loss of neutral conductor (at the upstream network) occurs (and by considering an unbalanced load), phase voltage imbalances take place, which can be detected by the voltage monitor device. The main drawback of this device is that it fails to detect the loss of neutral in cases of almost balanced loads (which is going to be a frequent condition in modern ZEBs, as discussed above) [2].

Another passive detection method is mentioned in [13] and it is based on the following.

1) The estimation of the zero-sequence impedance $z_{0,50Hz}$ at the fundamental frequency of the upstream network, when sufficient current passes through the neutral conductor.
2) The monitoring of the zero-sequence voltage v_0 of the upstream network.

The system diagnoses the fault of neutral loss when $z_{0,50Hz}$ or v_0 surpasses the predetermined limits. However, as in the case of the simple voltage monitor device, this system fails to detect neutral loss under almost balanced load per phase.

B. ISLANDING DETECTION

DERs inject their produced power in the grid and in combination with energy storage units, they compose microgrids. A microgrid can operate either in a grid-tied, or islanded operation. In the first case, the microgrid is capable of exchanging power with the mains, depending on local load values. On the other hand, in the islanded operation, DER should be capable of matching the generated power with the local power demand. In this regard, an islanding condition can be intentional or unintentional [6]. Intentional islanding is performed for the sake of scheduled maintenance, or in cases where there are major disturbances at the grid side; whereas unintentional islanding may occur randomly due to faults or other uncertainties in the power system. Unintentional islanding tends to be a threat for the maintenance personnel, the users and the components of the electrical installations.

Local islanding detection methods (at the DER-inverter level) are classified into passive and active ones. In passive schemes [6], [7], [8], islanding detection is achieved by monitoring significant deviations into the system output parameters, such as the voltage level or the frequency. The main advantage of passive detection schemes is that they do not cause any power quality issues; on the other hand, they suffer from wide NDZs and slow detection speeds.

Active methods are based on the injection of a small disturbance at the PCC [6]; by the aid of a positive feedback loop, this injection brings significant variations at the system parameters (i.e., frequency, voltage, and phase angle), under the islanding condition. Thus, active techniques can effectively detect islanding, even under load-matching conditions. On the other hand, they provoke power quality issues and therefore, the system performance may be degraded.

C. METER TAMPERING

Electricity theft is of major concern in Energy Markets, being an obstacle towards their growing path [15]. It is indicative that the reported cases related to meter tampering in Greece have reached 11 528 in 2016 [16]. Apart from the economic aspects, electricity theft results in a rise of the nonpredicted load, causing problems in the power system equipment and, consequently, it impacts on the grid voltage profile.

The most common meter tampering technique is the current bypassing, where a metal object is placed against the meter terminal block [17], [18]. This object forms a current divider with the current sensing circuit, causing the metal object to bypass a significant current amount, leading so to a smaller energy billing.

Smart meters deal with current bypassing tampering techniques, by measuring both the phase and the neutral currents, in order to detect cases of phase current bypassing. However, in case that bypassing actions regard both the neutral and the phase currents, the detection of meter tampering attempts becomes very difficult.

III. PRESENTATION OF THE PROPOSED ACTIVE DETECTION METHODOLOGY

A. SYSTEM ANALYSIS

The proposed detection scheme can detect islanding conditions, neutral loss, and also meter tampering attempts (current bypassing techniques, as stated in Section II-C). In the present analysis, the installation grounding system is considered to be of TN-S type, in a 3 ph system. The detection circuit consists of the following:

1) a voltage harmonic injection circuit;
2) a diagnosis system.

B. VOLTAGE HARMONIC INJECTION CIRCUIT

The voltage harmonic injection circuit generates a 12th-order (zero-sequence) harmonic voltage component, that is connected in series with the installation phase conductors. The selection of the 12th harmonic order is made for practical reasons, i.e., it is an unusual harmonic order in power grids and thus any interference in measurements is mostly avoided. In parallel, for the 12th harmonic component the relevant power quality standard, i.e., EN 50160 [19], which is the main document for the EU dealing with power quality, regarding the supplier side (at the PCC), does not foresee the presence of harmonic distortion (i.e., only 0.5% for even harmonics is permitted, from 6th up to 24th order). In this regard, the advantage of the acceptable harmonic level at this order is exploited, to make effective impedance estimations, without any need for inducing considerable amounts of voltage distortion. Moreover, in case of existing communication protocols in the electrical installation that may overlap with the specific harmonic injection, the proposed algorithm may as well operate by using another harmonic order (e.g., 14th, 16th, or a higher one), as long as it has the same features (being free from harmonic distortion from typical electrical equipment), remaining within the EN 50160 predefined limits [19]. It is worth noting that the provoke of additional issues at neighboring installations that use the proposed protection methodology is rather improbable, thanks to the fact that the harmonic injection is achieved by means of the development of high impedance voltage sources (a feature that provides the necessary isolation among neighboring harmonic injections).

In the general case of an M-phase system, the fault detection circuit incorporates M parallel branches that are connected in parallel with the phase loads of the installation. Each parallel branch includes one switching element, connected in series with a capacitor. These parallel branches ensure that sufficient amount of harmonic current can flow (i.e., they serve as a low impedance path at the selected harmonic order), leading to correct impedance estimations, even under no load conditions; once again, the selection of the 12th harmonic order is rather beneficial, as it also facilitates the use of compact film or ceramic capacitors. A schematic diagram

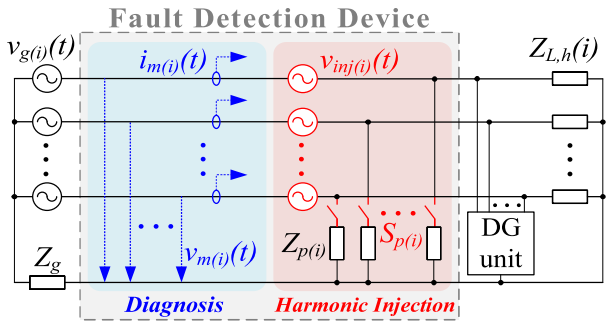

FIGURE 1. Overview of the proposed fault detection device in an M-phase electrical installation.

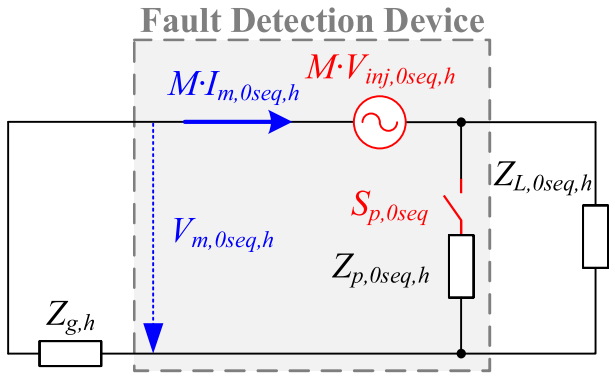

FIGURE 2. Equivalent harmonic (zero-sequence) model of the system.

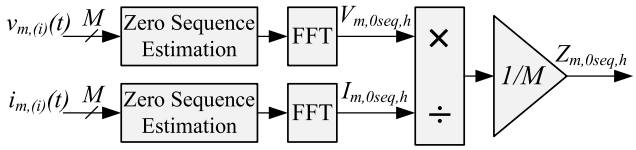

FIGURE 3. Block diagram of zero-sequence impedance estimation.

of the proposed fault detection device in generalized, M-phase electrical installation is depicted in Fig. 1. The grid phase voltages are described by the following expressions:

$$v_{g(i)}(t) = \sqrt{2}A_g \sin\left[\omega_g t + \varphi(i)\right] \tag{1}$$

$$\varphi(i) = \frac{2\pi}{M} i$$

$$\text{for } i = 1, 2, \ldots M \tag{2}$$

where A_g denotes the amplitude of the grid voltage, ω_g is the grid frequency, and M is the number of the phases of the system.

The mathematical expression that describes the continuous h_{th} harmonic voltage injection for each phase is

$$v_{inj}(i,t) = \sqrt{2}A_{inj}(i)\sin\left(h\omega_g t\right). \tag{3}$$

In the case of discontinuous harmonic voltage injection, of various harmonic components, the expression becomes

$$v_{inj}(i,k,t) = \left(\sum_{k=1}^{Q}\left[u(t-t_{i,k}) - u(t-\Delta t_{i,k}-t_{i,k})\right]\right) \cdot \left(\sqrt{2}A_{inj}(i,k)\sin\left(h(k)\omega_g t\right)\right) \tag{4}$$

where $i = 1, 2, \ldots M$ and $k = 1, 2, \ldots Q$

Q: The total number of the injected harmonic components.

$A_{\text{inj}}(i,k)$: The amplitude of the injected voltage components.

$t_{i,k}$: The starting time point of the $h(k)$ harmonic injection at the ith branch.

$\Delta t_{i,k}$: The time period of the $h(k)$ harmonic injection, of the ith branch.

C. EQUIVALENT ZERO-SEQUENCE MODEL

This Section presents the equivalent hth harmonic order (zero-sequence) model of the system, which is depicted in Fig. 2. The symbols in Fig. 3 are the following ones.

$Z_{g,h}$: The magnitude of the h-harmonic (zero-sequence) impedance of the grid.

$I_{m,h}$: The magnitude of the injected h-harmonic (zero-sequence) current.

$V_{m,0\text{seq},\,h}$: The measured h-harmonic (zero-sequence) voltage.

$S_{p,eq}$: The controllable switch for the harmonic path (it can be implemented by typical, bidirectional semiconductor switches, i.e., TRIACs).

The hth harmonic zero-sequence impedance component of the load is calculated by the following expression:

$$Z_{L,0seq,h} = \frac{\prod_{i=1}^{M} Z_{L,h}(i)}{\sum_{i=1}^{M}\left(\prod_{k=1,k\neq i}^{M}\left(Z_{L,h}(k)\right)\right)}. \tag{5}$$

In the same manner, the hth harmonic zero-sequence impedance component of the M parallel branches is calculated by the following expression:

$$Z_{p,0seq,h} = \frac{\prod_{i=1}^{M} Z_{p,h}(i)}{\sum_{i=1}^{M}\left(\prod_{k=1,k\neq i}^{M}\left(Z_{p,h}(k)\right)\right)}. \tag{6}$$

Considering (3) and (4), the equivalent harmonic zero-sequence voltage source is given by the following equations (for the cases of continuous and discontinuous injection modes, respectively)

$$v_{inj,0seq}(t) = \frac{1}{M}\sum_{i=1}^{M}\left(v_{inj}(i,t)\right) \tag{7}$$

$$v_{inj,0seq}(t) = \frac{1}{M}\sum_{i=1}^{M} v_{inj}(i,k,t). \tag{8}$$

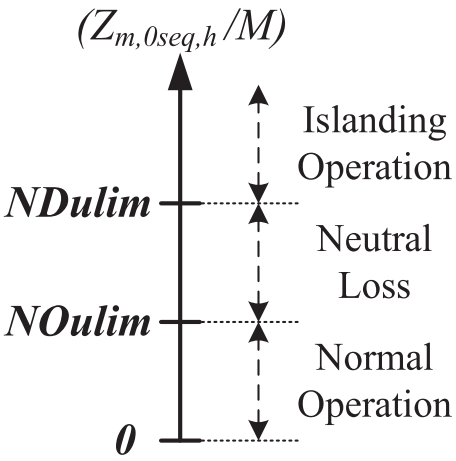

FIGURE 4. Fault-detection by monitoring the zero-sequence impedance.

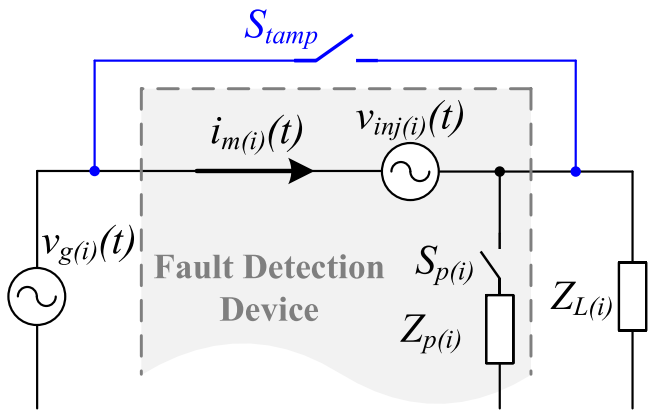

FIGURE 5. Overview of the equivalent circuit in case of meter tampering via current bypassing.

Finally, the magnitude of the hth harmonic zero-sequence injection current becomes

$$I_{inj,0seq,h} = \frac{1}{M}\frac{V_{inj,0seq,h}}{Z_{g,h} + Z_{p,0seq,h}//Z_{L,0seq,h}}. \quad (9)$$

D. DETECTION METHODOLOGY

1) ANTI-ISLANDING–NEUTRAL LOSS DETECTION SCHEME

Islanding conditions as well as neutral loss can be detected via the estimation of the zero-sequence grid impedance, using some mature tools such as DFT, FFT, Goertzel algorithm, etc. [6].

The estimation of the zero-sequence grid impedance, $Z_{m0seq,h}$, requires the measurement of voltage $v_{m(i)}$ and current $i_{m(i)}$ in every phase, as stated in Fig. 1 and described in (10)–(12). The procedure to estimate $Z_{m,0seq,h}$, which is based on the FFT method, is also presented in Fig. 3. It is worth noting that the utilization of the FFT algorithm is indicative, for the sake of the system functionality validation. Less computationally demanding algorithms (such as the Goertzel one) can be implemented as well

$$V_{m,0seq,h} = FFT_h\left(\frac{1}{M}\sum_{i=1}^{M} v_{m(i)}\right) \quad (10)$$

$$I_{m,0seq,h} = FFT_h\left(\frac{1}{M}\sum_{i=1}^{M} i_{m(i)}\right) \quad (11)$$

$$Z_{m,0seq,h} = \frac{V_{m,0seq,h}}{I_{m,0seq,h}} \quad (12)$$

where $v_{m,(i)}$ and $i_{m,(i)}$ are the measured voltage and current values of the ith phase.

The detection of neutral loss and islanding operation is based on the zero-sequence grid impedance assessment, as it is described in Fig. 4.

It is noted that the definition of the NO_{ulim} limit requires experimental testing, in which the noise and the accuracy of the measuring instruments should be taken into account. Furthermore, the ND_{ulim} limit is defined by considering a realistic range of values that the ground resistance can obtain in case of neutral loss. Above this value, islanding operation is considered for the system. For the sake of our analysis, the predetermined values of NO_{ulim} and ND_{ulim} are 20 and 50 Ω, correspondingly.

The aforementioned thresholds can be defined through measurements and practical assumptions, regarding the grounding resistance values of building installations. Specifically, the NO_{ulim} corresponds to realistic grounding resistance values, in cases of loss of neutral for the experimental setup, whereas the ND_{ulim} corresponds to practical impedance values of islanded loads. It is worth noting that these limits can be adapted to the specific features of the installations under consideration.

2) METER TAMPERING DETECTION SCHEME

Meter tampering via current bypassing is illustrated in Fig. 5; it involves the current bypass, through an external switch, S_{tamp}, one per phase of the installation. However, thanks to the proposed scheme, such an action results in a short circuit of the induced harmonic voltage source (of every bypassed phase), $v_{\text{inj}(i)}(t)$, leading so to short-circuit currents and voltage sags, at the selected harmonic order

$$I_{m(i)} = I_{inj(i)} = I_{inj,SC} \quad (13)$$

$$V_{inj(i)} = V_{inj,SC} \quad (14)$$

$I_{inj(i)}$: The magnitude of the hth harmonic injected current.
$I_{inj,SC}$: The magnitude of the hth harmonic short circuit current.
$V_{inj,SC}$: The magnitude of the hth harmonic voltage source when the switch S_{tamp} is closed.

Hence, according to this detection scheme, in case that $I_{m,0\text{seq},h}$ exceeds the threshold value of $I_{SC,thr}$, a meter tampering attempt is considered.

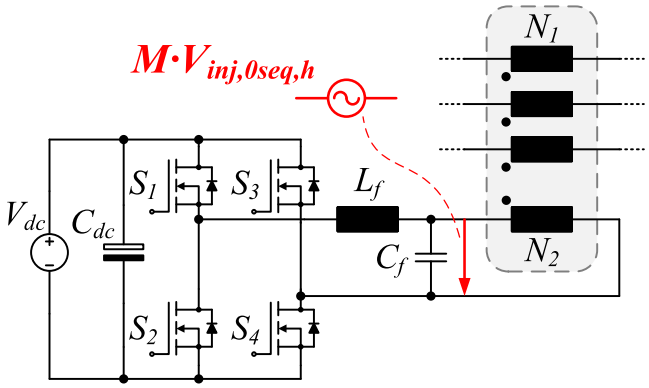

FIGURE 6. Equivalent zero-sequence voltage source model.

E. EQUIVALENT CIRCUIT OF THE HARMONIC (ZERO-SEQUENCE) VOLTAGE SOURCE

The equivalent model of the zero-sequence harmonic voltage source, $M \cdot v_{inj,0seq,h}$, which has been analyzed in Section III-C, consists of the following.

1) A current transformer with M primary and one secondary windings.
2) A harmonic voltage source.

The primary (low impedance) windings of the current transformer are connected in series with the installation phase conductors, whereas the harmonic voltage generator supplies the secondary (high impedance) winding, as it is depicted in Fig. 6. In such a way, when voltage injection takes place, the power flow at the fundamental frequency (50 or 60 Hz) is not affected. In addition, this implementation needs less components than in the case of using M separate current transformers and M harmonic voltage sources.

The harmonic voltage generator may consist of any type of voltage inverter topology, such as the H-bridge inverter, which has been selected in this work. The harmonic voltage signal is modulated by the aid of SPWM technique.

F. POSSIBLE ALTERNATIVE CONFIGURATION OF THE PROPOSED DETECTION SCHEME

In this section, some alternative configurations of the proposed detection scheme are presented, which simplify its circuitry, in case that tampering detection is not mandatory.

1) The zero-sequence harmonic current can be measured by only one current sensor (instead of M), by placing it at the neutral conductor, resulting so in fewer components and less computational cost.
2) The injection of the zero-sequence harmonic voltage can be implemented by using a current transformer with only one primary winding that is connected in series with the neutral conductor. In this way, the number of primary windings is limited from M to one; thus, the current transformer design becomes rather simple.

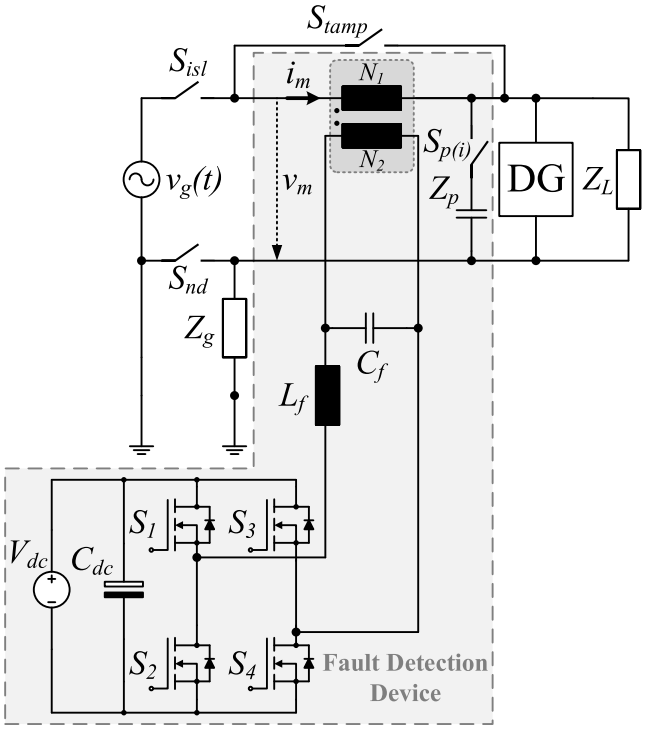

FIGURE 7. Simulation of the proposed fault detection scheme in case of a 1 ph electrical installation.

G. AREA OF APPLICATION

The application area of the newly proposed fault detection scheme includes all residential, commercial, and industrial building infrastructures with/without DG installations. The proposed fault detection scheme can be integrated either in the circuit of a smart meter, or it can operate in coordination with any pre-existing energy meter in the infrastructure, providing fault indications.

Last but not least, it is worth noting that the main features of the proposed device that can be exploited centrally, at Medium to Low Voltage (MV/LV) substation level, is the effective unintentional islanding and neutral conductor loss detection, by its series connection (through appropriate current transformers) at the LV feeders. In parallel, as the proposed system detects meter tampering at local (installation) level, it may facilitate indirect detection methods as well, applied at central (MV/LV substation) level, which are based on consumer load profile data monitoring [20], exploiting available data from consumer installations.

IV. SIMULATION RESULTS

The simulation model of the aforementioned fault detection circuit is presented in Fig. 7 [in its single phase (1 ph) version]; the simulation process demonstrates the operational features of the proposed scheme, both for the cases of 1 ph and 3 ph systems. The detection circuit consists of an H-bridge inverter, which is connected at the secondary winding of a

TABLE 1. Main Parameters of the Simulated and Experimental System

Parameter (description)	Value [unit]
V_{dc}	70.7 [V]
$V_{g,rms}$ (rms grid voltage value, phase-to-ground)	230 [V]
f_{grid} (fundamental frequency)	50 [Hz]
f_{inj} (frequency of the injected component)	600 [Hz]
Injection period T_{inj}	0.4 [s]
Injection time $t_{on,inj}$	0.2 [s]
Impedance estimation method	FFT
C_p	4.4 [μF]
N1:N2	1:20
f_{sw} (SPWM switching frequency)	100 [kHz]
L_f	0.12 [mH]
C_f	2.2 [μF]
NO_{Ulim}	20 [Ω]
ND_{Ulim}	50 [Ω]

current transformer. The inverter uses SPWM to modulate the 12th-order harmonic voltage component. The primary winding/s is/are connected in series with the phase conductor(s). The detection device comprises also one/three parallel branches, i.e., a power switch, connected in series with a capacitor, providing the necessary low impedance harmonic path per phase, in case of no-load conditions.

The impedance estimation method is based on the FFT algorithm and the average value of the zero-sequence impedance $z_{m,0seq,h}$ is calculated, at the end of every injection period. The fault of neutral conductor loss is simulated by adding resistor z_g, via the deactivation of switch S_{nd}. In normal operation the switch S_{nd} is ON, creating so a zero-impedance path for the current at the neutral conductor; otherwise, the neutral path presents the high resistance value z_g. The meter tampering via the current bypassing technique is simulated by the aid of the switch S_{tamp}, which is OFF in normal operation and on when tampering occurs. Finally, the islanded operation is applied by the deactivation of switch S_{isl}. The DG unit incorporates a 1 ph/3 ph H-bridge inverter, which transfers the generated active power, P_{dc}, to the installation; the inverter is controlled by the aid of a commonly used instantaneous pq algorithm.

The main parameters of the simulated system are summarized in Table 1. It is noted that these parameters are valid for the experimental system too, which is described in Section V.

A. SINGLE PHASE SYSTEM

The simulated 1 ph system, which is depicted in Fig. 6, is examined under three different fault scenarios (i.e., neutral loss, islanding, meter tampering).

1) NEUTRAL LOSS (SINGLE PHASE ELECTRICAL INSTALLATION)

In the neutral loss simulation scenario, the power of the load is $P_L = 1{,}058$ W, whereas the ground resistance is considered to be $Z_g = 30\ \Omega$; for the sake of simplicity, the operation of the DG unit is suspended. The fault occurs at 0.8 s and the system estimates the average value of the impedance $z_{m,0seq,h}$ at the end of the injection time. As it is evident from Fig. 8,

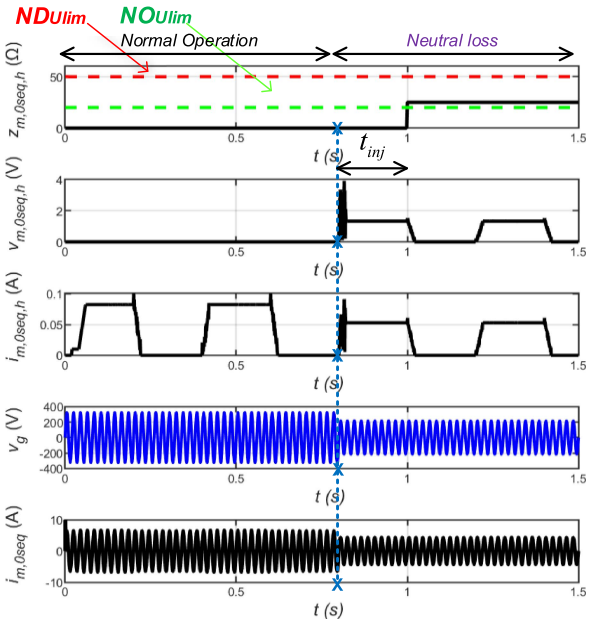

FIGURE 8. Simulation waveforms: Zero-sequence harmonic impedance, injected voltage and current, grid voltage and zero-sequence current in case of neutral loss in a 1 ph electrical installation ($P_L = 1058$ W, $Z_g = 30\ \Omega$).

the impedance value exceeds NO_{Ulim}, due to the loss of neutral conductor, and thus the fault detection is successful.

2) ISLANDING OPERATION (SINGLE PHASE ELECTRICAL INSTALLATION)

In the islanding simulation scenario, the load is composed of parallel RLC elements, rated at $P_L = 1{,}058$ W with $QF = 1$, under load-matching conditions (the DG unit operates at $P_{DG} = 1{,}058$ W). Simulation results for the islanding detection scenario are presented in Fig. 9. The fault occurs at 0.8 s and the system estimates mean value of the impedance $z_{m,0\text{seq},h}$ at the end of the injection time. The value of $z_{m,0\text{seq},h}$ exceeds ND_{Ulim} under islanded operation; therefore the fault detection is successful.

3) METER TAMPERING (SINGLE PHASE ELECTRICAL INSTALLATION)

In the meter tampering simulation scenario, the power of the load is $P_L = 1058$ W, whereas for the sake of simplicity, the operation of the DG unit is suspended. Meter tampering occurs at 0.8 s, provoking a zero-sequence harmonic current value over the predetermined limit of $I_{SC,thr} = 30$ A, indicating so a meter tampering event. Simulation results for the meter tampering case in a 1 ph installation are illustrated in Fig. 10.

B. THREE PHASE SYSTEM

The simulation of the 3 ph system, depicted in Fig. 11, is examined under three different fault scenarios (neutral loss, islanding, meter tampering).

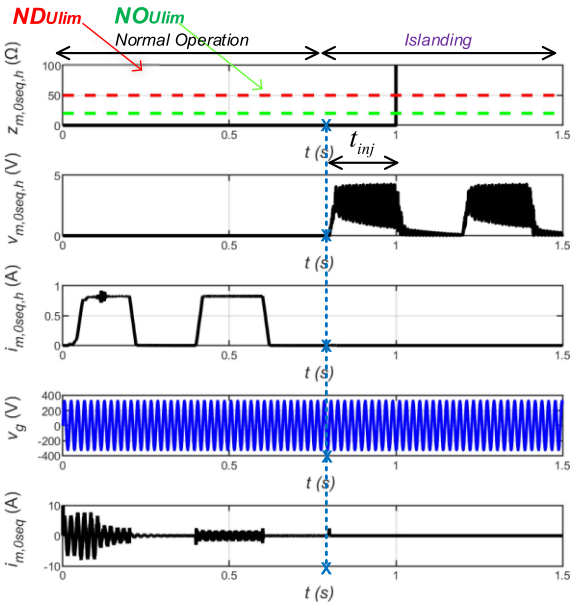

FIGURE 9. Simulation waveforms: Zero-sequence harmonic impedance, voltage and current, grid voltage and zero-sequence current in case of islanded operation of a 1 ph electrical installation ($P_L = 1058$ W, $QF = 1$, $P_{DG} = 1058$ W).

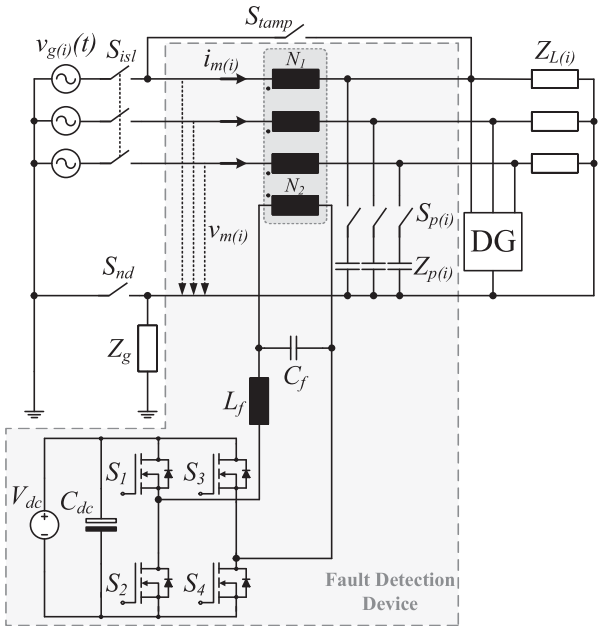

FIGURE 11. Simulation of the proposed fault detection scheme in case of a 3 ph electrical installation.

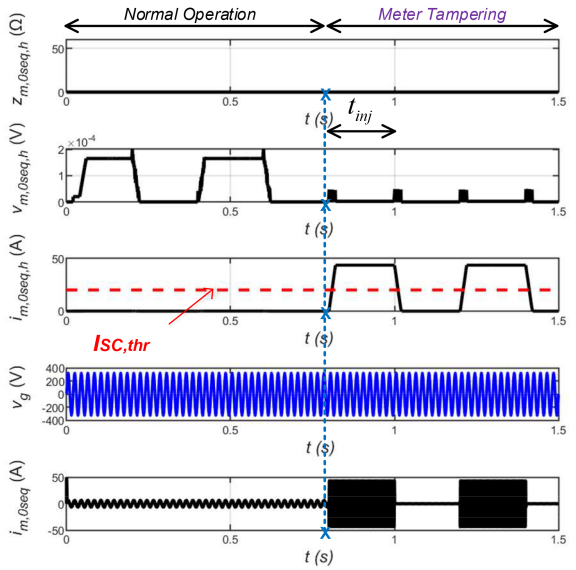

FIGURE 10. Simulation waveforms: Zero-sequence harmonic impedance, voltage and current, grid voltage, and zero-sequence current in case of a meter tampering via the current bypass technique, in a 1 ph electrical installation ($P_L = 1058$ W).

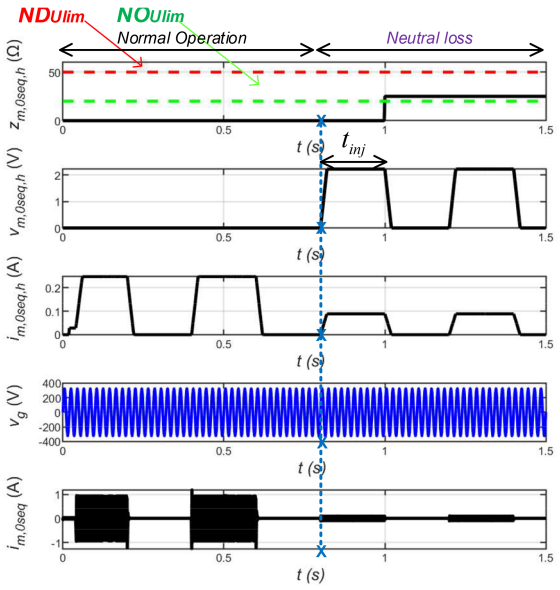

FIGURE 12. Simulation waveforms: Zero-sequence harmonic impedance, voltage and current and grid voltage, zero-sequence current in case of Neutral loss in a 3 ph installation ($P_L = 1058$ W/ph, $Z_g = 30$ Ω).

1) NEUTRAL LOSS (THREE PHASE ELECTRICAL INSTALLATION)

In the neutral loss simulation scenario, the power of the load is $P_L = 1058$ W/ph, the ground resistance $Z_g = 30$ Ω and the operation of the DG unit is suspended. In Fig. 12 simulation results for the neutral loss scenario are presented. The fault occurs at 0.8 s and the system estimates the mean value of the impedance $z_{m,0\text{seq},h}$ at the end of the injection time. The value of $z_{m,0\text{seq},h}$ is placed between the NO_{Ulim} and the ND_{Ulim}, indicating so the fault of neutral conductor loss.

2) ISLANDING OPERATION (THREE PHASE ELECTRICAL INSTALLATION)

For the islanding operation case, simulation results are depicted in Fig. 13.

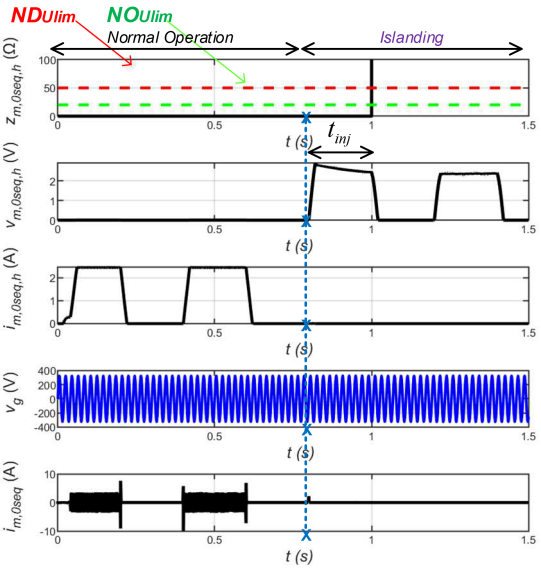

FIGURE 13. Simulation waveforms: Zero-sequence harmonic impedance, voltage and current, grid voltage and zero-sequence current in case of islanded operation in a 3 ph installation ($P_L = 1058$ W/ph, $QF = 1$, $P_{DG} = 1058$ W/ph).

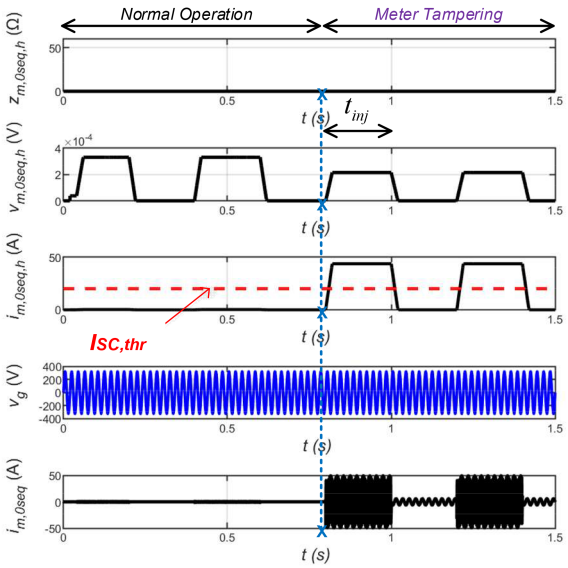

FIGURE 14. Simulation waveforms: Zero-sequence harmonic impedance, voltage and current, grid voltage and zero-sequence current in case of meter tampering via the current bypass technique (phase a) in a 3 ph installation.

In the simulation scenario, the load is composed of 3 parallel RLC elements rated at $P_L = 1058$ W/ph with $QF = 1$, whereas the 3 ph DG unit operates also at $P_{DG} = 1058$ W/ph (load matching conditions). The fault occurs at 0.8 s and the system estimates the mean value of the impedance $z_{m,0\text{seq},h}$ at the end of the injection time. After islanding occurs the value of $z_{m,0\text{seq},h}$ exceeds ND_{Ulim}; hence, the fault detection is successful.

3) METER TAMPERING (THREE PHASE ELECTRICAL INSTALLATION)

Finally, in the meter tampering simulation scenario, the load power is $P_L = 1058$ W/ph, whereas, for the sake of simplicity, the operation of the DG unit is suspended. Simulation results for this scenario are presented in Fig. 14. Meter tampering occurs at 0.8 s at phase a, leading the zero-sequence harmonic current over the threshold value of 30 A, and thus the meter tampering attempt is successfully detected.

V. EXPERIMENTAL RESULTS

To experimentally verify the proposed detection scheme (regarding the faults of neutral loss and meter tampering in 1 and 3 ph electrical installations), a prototype H-bridge inverter has been designed and constructed, along with a current transformer; an overview of the 1/3 ph experimental model is illustrated in Fig. 15, whereas the laboratory test bench is depicted in Fig. 16(a). The current transformer is connected in series with the neutral conductor of the installation, as it is described in Section III-E. A practical device implementation (compact industrial prototype) is also depicted, in Fig. 16(b), indicating the feasibility of the proposed solution.

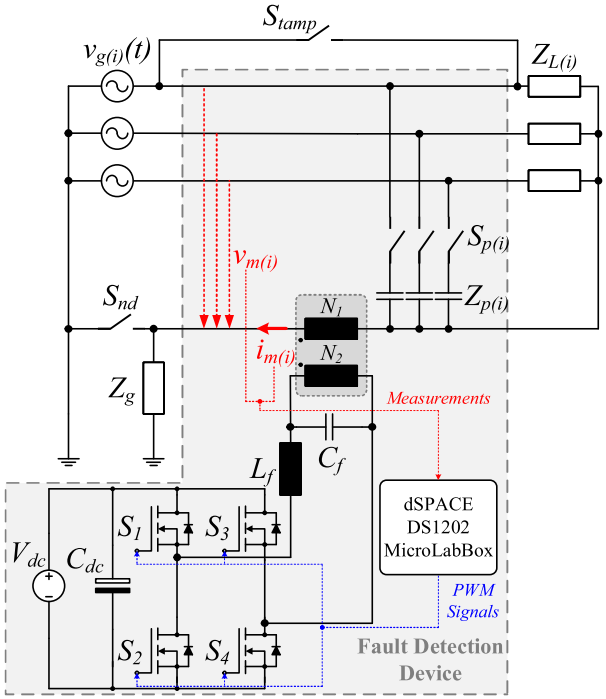

FIGURE 15. Schematic diagram of the 1 ph/3 ph experimental system.

Furthermore, a parallel branch is connected at each phase. In this implementation, switches $S_{p(i)}$ (TRIAC devices) remain active for the whole injection period T_{inj}. One/Three voltage transformers are used to monitor the grid side voltage. The zero-sequence current measurements are acquired by a current probe (Tektronix TCPA300) at the neutral conductor.

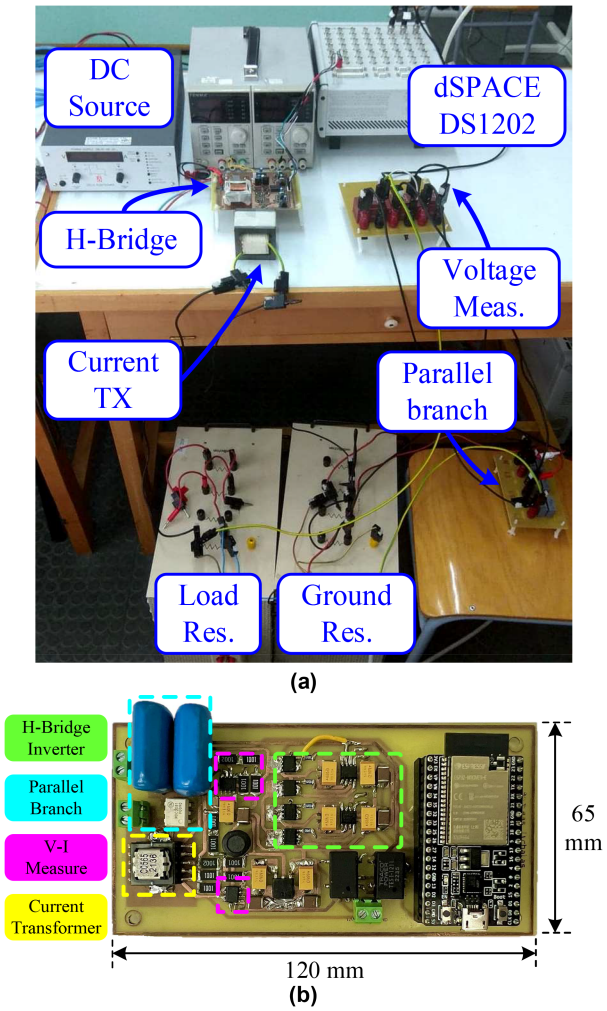

FIGURE 16. (a) Overview of the 3 ph experimental setup. (b) Compact industrial prototype.

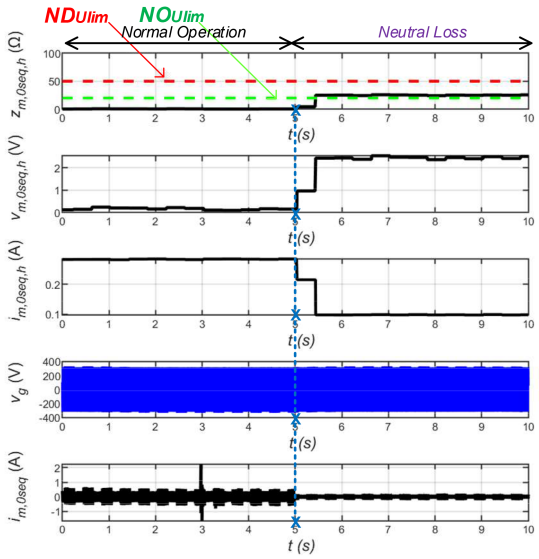

FIGURE 17. Experimental waveforms: Zero-sequence harmonic impedance, voltage and current, grid voltage and zero-sequence current in case of Neutral loss in a 3 ph installation ($P_L = 1058$ W/ph, $Z_g = 25$ Ω).

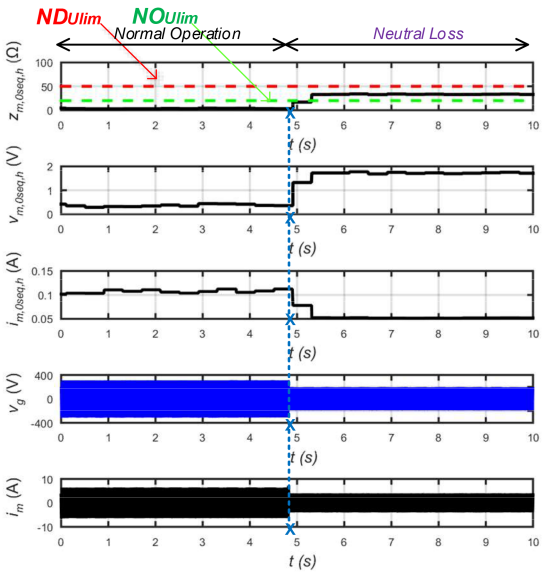

FIGURE 18. Experimental waveforms: Zero-sequence harmonic impedance, voltage and current, grid voltage and zero-sequence current in case of neutral loss in a 1 ph installation ($P_L = 1058$ W, $Z_g = 25$ Ω).

The dSPACE MicroLabBox (DS1202) system is used, to extract the harmonic zero-sequence voltage, current and impedance, as well as to drive the H-bridge inverter, via the SPWM technique.

The parameters of the experimental system are described in Table 1. It is noted that for the sake of the experimental validation, the setup may operate either in 3 ph or in 1 ph mode.

Figs. 17 and 18 depict the waveforms of the monitored harmonic impedance, voltage and current, as well as the grid voltage and the zero-sequence current, at the fundamental frequency, for a 3 ph and a 1 ph electrical installation, respectively. The fault of neutral conductor loss occurs at 5 s and the load active power and the ground resistance are considered $P_L = 1058$ W/ph and $Z_g = 25$ Ω, correspondingly. The value of $z_{m,0\text{seq},h}$ comes between ND_{Ulim} and NO_{Ulim}, indicating so the fault of neutral loss. This experimental case highlights that the proposed detection scheme is capable of detecting the fault of neutral loss even under load matching conditions, in contrast to the commercial voltage monitor devices—as stated in Section II-A.

Next, the neutral loss detection is tested under no load conditions (3 ph installation); Fig. 19 illustrates the waveforms of the monitored harmonic impedance, voltage and current, as well as the grid voltage and the zero-sequence current at the fundamental frequency. Once again, the fault of neutral loss occurs at 5 s and the value of the ground resistance is considered to be $Z_g = 25$ Ω. Due to the no load condition, the parallel branch is activated, providing so a low-impedance

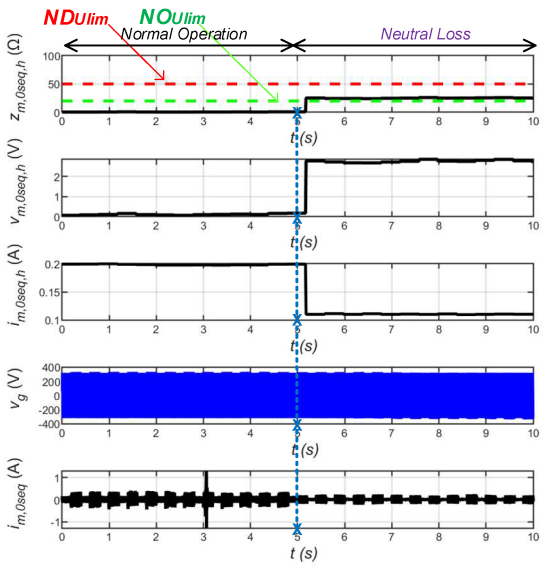

FIGURE 19. Experimental waveforms: Zero-sequence harmonic impedance, voltage and current, grid voltage and zero-sequence current in case of neutral loss in a 3 ph installation ($P_L = 0$ W/ph, $Z_g = 25$ Ω).

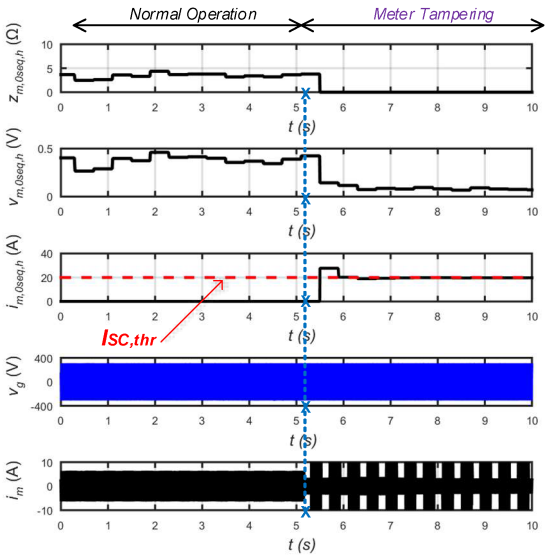

FIGURE 20. Experimental waveforms: Zero-sequence harmonic impedance, voltage and current, grid voltage and zero-sequence current in case of meter Tampering via the current bypass technique in a 1 ph installation ($P_L = 1058$ W, $Z_g = 0$ Ω).

path for the injected harmonic current. As in the previous case, the calculated impedance value of $z_{m,0\text{seq},h}$ comes between ND_{Ulim} and NO_{Ulim}, indicating the fault of neutral loss.

In Figs. 20 and 21, the waveforms of the monitored harmonic impedance, voltage, and current, as well as the grid voltage and the zero-sequence current at fundamental frequency are depicted, in case of a meter tampering attempt via the current bypassing technique (1 ph installation). Specifically, this incident occurs at 5 s for $P_L = 1058$ W and without load, accordingly. The value of the ground resistance is considered to be $Z_g = 0$ Ω. According to those experimental

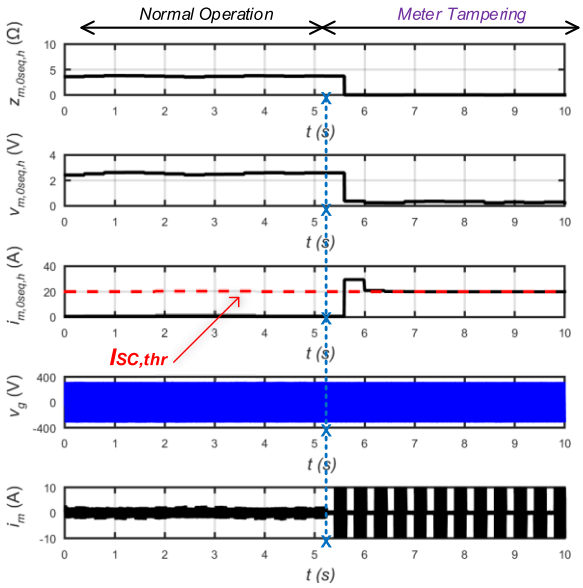

FIGURE 21. Experimental waveforms: Zero-sequence harmonic impedance, voltage and current, grid voltage and zero-sequence current in case of meter tampering via the current bypass technique in a 1 ph installation ($P_L = 0$ W, $Z_g = 0$ Ω).

results, the detection of this tamper metering attempt is in both cases successful, as the value of the zero-sequence harmonic current $i_{m0seq,h}$ becomes high, exceeding the threshold value ($I_{SC,thr}$) of 20 A.

VI. CONCLUSION

An active protection scheme for modern electrical installations is proposed, capable of detecting neutral loss, unintentional islanding, and meter tampering. The proposed concept periodically injects a series zero-sequence harmonic voltage component, at the phases of the electrical installation and by monitoring the zero-sequence harmonic impedance and current it diagnoses and classifies the fault type. In addition, a suitable technical solution is proposed, regarding the implementation of the series zero-sequence harmonic voltage injection in an M-phase system, without affecting the power flow of the installation at the fundamental frequency, by using a single current transformer. Furthermore, a solution about the impedance estimation under no load conditions is provided, by placing a parallel branch in each phase of the installation, which comprises a TRIAC switch, in series with a capacitor. The effectiveness of the proposed scheme is studied and validated through simulations and experiments at a 1 ph/3 ph setup.

In contrast to the state-of-the-art methods, which are mostly based on the harmonic current injection, the proposed scheme utilizes a series zero-sequence harmonic voltage injection mechanism, providing a holistic solution regarding the issues of unintentional islanding and neutral loss, in the context of modern electrical installations and the prospect of mass installation of DGs and storage units. In parallel, the proposed

scheme is capable to detect any meter tampering attempt without any need of statistical or numerical methods, which introduce uncertainties. The proposed fault detection scheme is patent protected, *Patent ID: GR1009858 (B)*, and it can be integrated either in the circuit of a smart meter, or to operate in coordination with any pre-existing energy meter in the infrastructure, providing fault warnings.

REFERENCES

[1] A. Kyritsis et al., "Evolution of PV systems in Greece and review of applicable solutions for higher penetration levels," *Renewable Energy*, vol. 109, pp. 487–499, Aug. 2017.

[2] F. Kotarela, A. Kyritsis, N. Papanikolaou, and S. A. Kalogirou, "Enhanced nZEB concept incorporating a sustainable grid support scheme," *Renewable Energy*, vol. 169, pp. 714–725, May 2021.

[3] Directive 2018/844/EU 2010 European Parliament and of the Council of 30 May 2018 amending Directive 2010/31/EU. [Online]. Available: https://eur-lex.europa.eu/legal-content/EN/TXT/?uri=uriserv%3AOJ.L_.2018.156.01.0075.01.ENG

[4] S. Cui, Y.-W. Wang, J.-W. Xiao, and N. Liu, "A two-stage robust energy sharing management for Prosumer microgrid," *IEEE Trans. Ind. Informat.*, vol. 15, no. 5, pp. 2741–2752, May 2019, doi: 10.1109/TII.2018.2867878.

[5] B. Gu et al., "Optimal charge/discharge scheduling for batteries in energy router-based microgrids of prosumers via peer-to-peer trading," *IEEE Trans. Sustain. Energy*, vol. 13, no. 3, pp. 1315–1328, Jul. 2022, doi: 10.1109/TSTE.2022.3154145.

[6] F. Valsamas, D. Voglitsis, N. Rigogiannis, N. Papanikolaou, and A. Kyritsis, "Comparative study of active anti-islanding schemes compatible with MICs in the prospect of high penetration levels and weak grid conditions," *Inst. Eng. Technol. Gener. Transmiss. Distrib.*, vol. 12, pp. 4589–4596, Nov. 2018, doi: 10.1049/iet-gtd.2018.5636.

[7] D. Voglitsis, F. Valsamas, N. Rigogiannis, and N. P. Papanikolaou, "On harmonic injection anti-islanding techniques under the operation of multiple DER-inverters," *IEEE Trans. Energy Convers.*, vol. 34, no. 1, pp. 455–467, Mar. 2019, doi: 10.1109/TEC.2018.2881737.

[8] D. Voglitsis, F. Valsamas, N. Rigogiannis, and N. Papanikolaou, "On the injection of sub/inter-harmonic current components for active anti-islanding purposes," *Energies*, vol. 11, no. 9, Aug. 2018, Art. no. 2183, doi: 10.3390/en11092183.

[9] *Low-Voltage Electrical Installations - Part 1: Fundamental Principles, Assessment of General Characteristics, Definitions*, Standard IEC 60364-1:2020, May 2020.

[10] *Utility-Interconnected Photovoltaic Inverters - Test Procedure of Islanding Prevention Measures*, Standard IEC 62116:2014, Feb. 2014.

[11] D. Y. Yamashita, I. Vechiu, J.-P. Gaubert, and S. Jupin, "Hierarchical model predictive control to coordinate a vehicle-to-grid system coupled to building microgrids," *IEEE Trans. Ind. Appl.*, vol. 59, no. 1, pp. 169–179, Jan./Feb. 2023, doi: 10.1109/TIA.2022.3215978.

[12] "Effect of neutral loss in 3-phase LV networks," *ABB Technical Journal*, pp. 1–4, Nov. 12.

[13] S. Frantzeskakis, D. Voglitsis, N. Papanikolaou, C. Christodoulou, and I. Gonos, "Loss of neutral in low voltage electrical installations with connected DG units - consequences and solutions," in *Proc. 25th Int. Conf. Electricity Distrib.*, 2019, pp. 1–5.

[14] M. H. Xivambu, "Impact of floating neutral in distribution systems," in *Proc. 19th Int. Conf. Electricity Distrib.*, 2007, pp. 21–24.

[15] P. Chandel, T. Thakur, and B. A. Sawale, "Energy meter tampering: Major cause of non-technical losses in Indian distribution sector," in *Proc. Int. Conf. Elect. Power Energy Syst.*, 2016, pp. 368–371, doi: 10.1109/ICEPES.2016.7915959.

[16] "Clarifications on the electricity theft phenomenon," HEDNO, Jan. 2018. [Online]. Available: https://www.deddie.gr/el/kentro-enhmerwsis/deltia-tupou/deltia-tupou-2018/ianouarios-2018/dieukriniseis-sxetika-me-to-fainomeno-twn-reumatok/

[17] S. Ngamchuen and C. Pirak, "Smart anti-tampering algorithm design for single phase smart meter applied to AMI systems," in *Proc. 10th Int. Conf. Elect. Eng./Electron., Comput., Telecommun. Inf. Technol.*, 2013, pp. 1–6, doi: 10.1109/ECTICon.2013.6559617.

[18] M. Mesganaw, "*How to Detect and Harden an Electricity Meter Against Tampering by Neutral Disconnection*. Dallas, Texas, USA: Texas Instruments, 2020, App. Note.

[19] European Standard, *Voltage Characteristics of Electricity Supplied by Public Electricity Networks*, European Committee for Electrotechnical Standardization (CENELEC), Standard EN 50160:2010, 2010.

[20] G. Messinis and N. Hatziargyriou, "Review of non-technical loss detection methods," *Electric Power Syst. Res.*, vol. 158, pp. 250–266, May 2018.

SYLLAS FRANTZESKAKIS received the Dipl. Eng. and M.Sc. degrees in electrical and computer engineering from the Democritus University of Thrace, Xanthi, Greece, in 2018 and 2020, respectively.

His research interests include the analysis, design, simulation, and development of dc/dc and dc/ac power converters for renewable energy systems and microgrid applications.

Prof. Frantzeskakis is a member of the Technical Chamber of Greece.

NICK RIGOGIANNIS (Member, IEEE) received the Dipl.Eng. and M.Sc. degrees in electrical and computer engineering from the Democritus University of Thrace, Xanthi, Greece, in 2017 and 2019, respectively. He is currently working toward the Ph.D. degree in power electronics.

His main research interests include power electronics, digital control of power converters, transportation electrification, renewable energy systems, and power quality. He has the authored and coauthored more than 40 scientific papers in his field, published in high quality Journals and Conference Proceedings. He has been involved in several research programs, both National-funded and European-funded, as well as in Industrial research projects.

Mr. Rigogiannis is a Member of IEEE Power Electronics Society (PELS), and a Member of CIGRE and the Technical Chamber of Greece.

CHRISTOS CHRISTODOULOU received the Dipl. Eng. and Ph.D. degrees in electrical engineering from the National Technical University of Athens, Athens, Greece, in 2006 and 2010, respectively.

Prior to his academic carrier, he had been working for several years in the Hellenic Electricity Distribution Network Operator—involved with distribution network planning as well as with several European distribution projects. He is currently an Assistant Prfessor with the School of Electrical and Computer Engineering, National Technical University of Athens, Greece. He has authored and coauthored more than 80 papers in scientific journals and conference proceedings.

His research interests include high voltages, lightning protection, distributed generation, electrical installations, energy saving, power quality improvement, and electromagnetic compatibility.

NICK PAPANIKOLAOU (Senior Member, IEEE) received the Dipl.Eng. and Ph.D. degrees in electrical engineering from the University of Patras, Patras, Greece, in 1998 and 2002, respectively.

Prior to his academic career, he had been working for several years in the Hellenic Electric Energy Industry—involved with major European transmission and generation projects. He is currently a Full Professor with the Department of Electrical and Computer Engineering, Democritus University of Thrace, Xanthi, Greece. His research interests include power electronics, renewable energy exploitation, distributed generation, energy saving, electric vehicles, and power quality improvement.

Dr. Papanikolaou is a Member of CIGRE and the Technical Chamber of Greece.